

3. RESULTS

Representative samples of spent printed circuit boards (PCBs) were visually inspected and analyzed. Table 3 shows the type of metals detected in these samples. Table 4 shows the weight percentage of these metals in the PCB samples.

Table 3 The composition of the spent PCBs

PCB type	color		Metal		
	Base	Coating	substrate	Deposited	Strips
a	Dark, brown and white polymer plate	Usually green	Copper	Tin-lead alloy	-
b	Yellowish polymer plate		copper	Copper	Gold
c	White polymer plate		-	Cu/Sn/Pb	Sn/Pb

Table 4 Average Composition of typical PCBs

Metal	%	
	Single side PCB	Double side PCB
Copper	15	25
Lead	2	3
Tin	2	3
Gold*	0.5	1.5
Base material	80.3	67.5

* In type c

Plates 7 through 18 show the photographs of the spent PCB samples. It can be seen that different types and categories of the spent boards are wasted in the scrap yard (Plate 7). Plates 8 – 10 represents a stripped parts of the mother plate before manufacturing. The strips have different size and color. Plate 12 shows a bed plate

made of polymeric material after making the required drawings and perforation system during PCB manufacture technology.

The photograph shows the wasted PCB that constitutes the major part of scrap. The light color represents the base material whereas the dark spots represent partially oxidized copper. The inner frame shows copper layer after printing and etching processes.

Plates 12 and 13 shows a scrap of printed circuit board after drilling and soldering with tin/lead alloy



Plate. 7A photograph of spent PCBs cut strips.

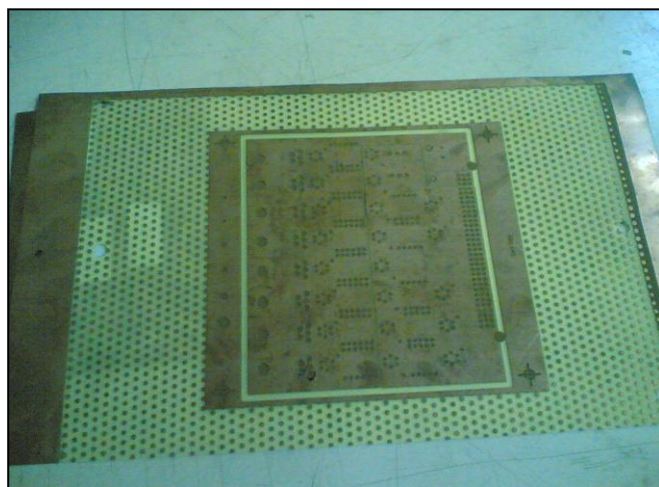


Plate 8 A photograph of a multilayer base material with copper (after print and etch) (the dark area at the preferential is out of use and will be removed)



Plate 9 The removed base material cut from the preferential as shown in plate 2.



Plate 10 A view of removed parts from the finished PCBs after final manufacturing.

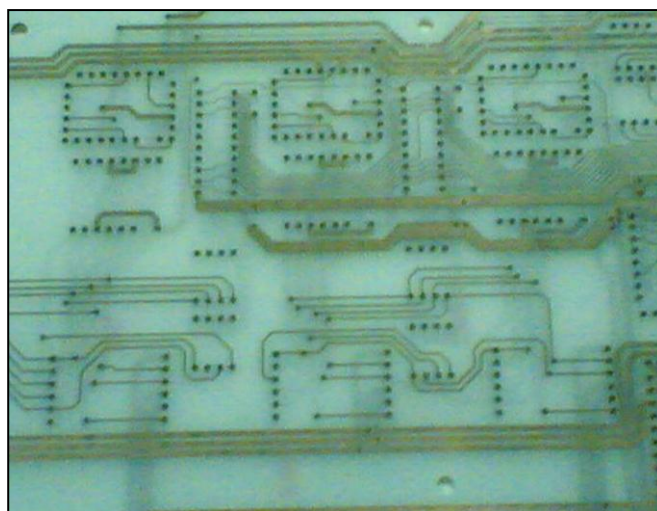


Plate 11 Bed plate made of polymeric material after making the required drawings and perforation.



Plate 12 PCB samples containing soldering material

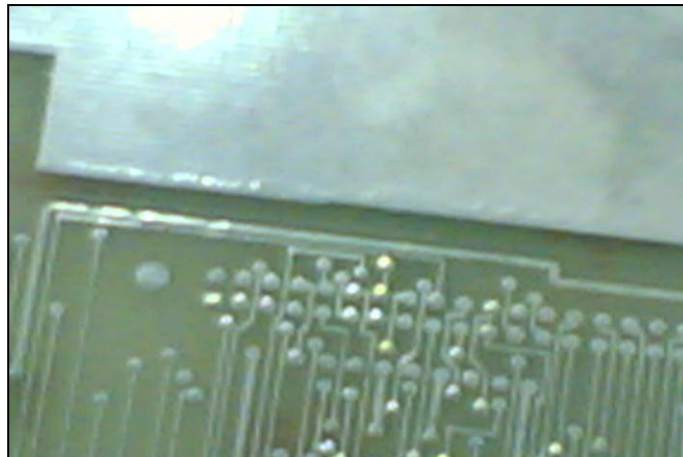


Plate13 PCB samples containing soldering material

Plate 14 and 15 shows the cut boundary of base plate after finishing and manufacturing the PCB. The green color represents the solder mask that coats a copper layer. In plate 9 the dark color represents the base material.

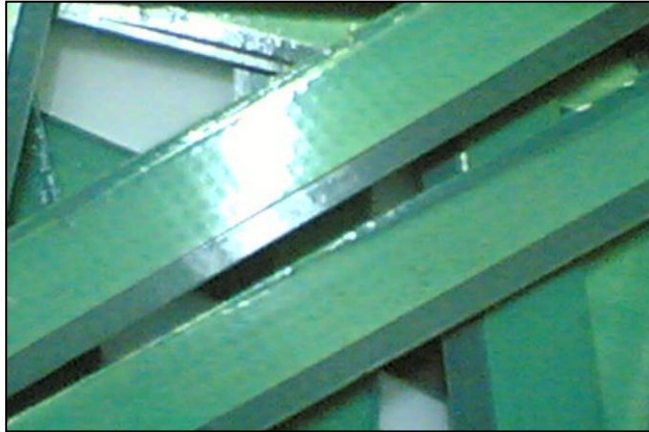


Plate 14 cut boundary pieces of finished PCB



Plate 15 Cut boundary pieces from finished multilayer PCB

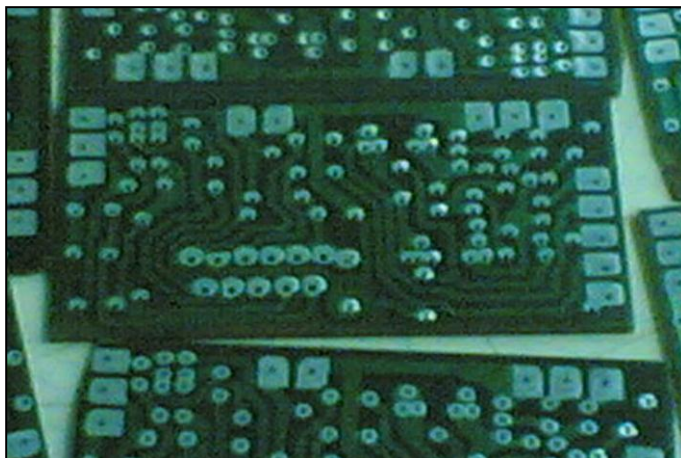


Plate 16 A scrap of finished PCB after drilling and soldering with Sn/Pb alloy

Plate 16 shows printed circuit board scrap after drilling and soldering with Tin/lead alloy. The dark color represents the base material coated with solder mask and the light green color represents the solder mask coated on copper layer whereas the white colored parts represents the tin / lead solder layer on copper layer.

Plate 17 shows scrap of PCB after drilling and soldering with Sn / Pb alloy. The yellow color represents gold fingers plated on copper. The green color shows the solder mask on base material while the white color represents the Sn/Pb solder.

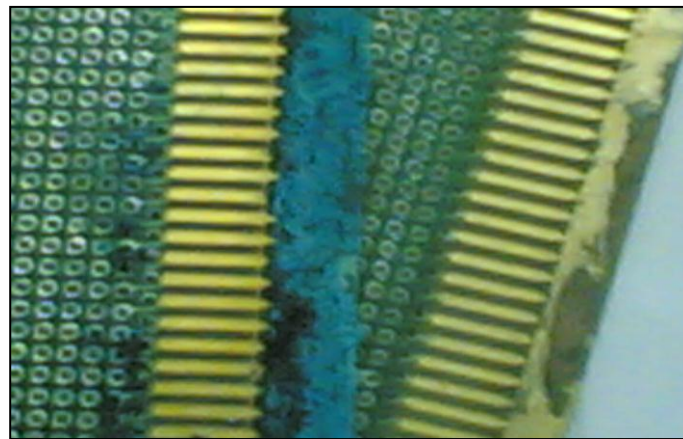


Plate 17 A scrap PCB containing Sn/Pb soldering and gold fingers.

Plate 18 shows PCB scrap containing gold plated on copper layer. The light color represents the base material while the dark color represents the gold layer coated on copper layer.

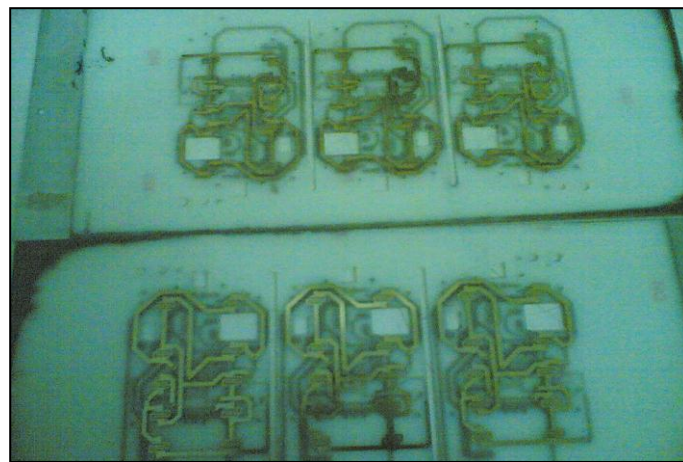


Plate 18 PCB scrap containing gold layer coated on copper

3.1 Extraction of metals from PCBs by pyrometallurgical treatment

Figure 2 shows the effect of heating the printed circuit boards scrap samples in open atmosphere and normal pressure on weight loss till constant loss value. At each temperature period, the sample was kept in the acid to get rid of the volatiles. It can be seen that during the early heating process, printed circuit boards scrap samples exhibit a non significant extent of weight loss (about 5% at 300°C). With further increase in heating temperature 600°C the extent of weight loss exhibits a drastic increase to achieve a value of about 60%. Within the temperature range 600 – 900°C a slight increase in weight loss takes place and a constant value is approached at >800°C.

3.1.1 Dissolving the ash of the PCB in sulfuric acid and HCl

Figure 3 shows the extent of dissolution in weight %, of the ash left behind burning the PCBs scrap, in sulfuric acid having different molarity at room temperature. It is seen that dissolution of the ash increases gradually with increase in time approaching a constant value after 50 minutes. Dissolution takes place more readily with concentrated sulfuric acid (>3M) as compared to the diluted acid solution (<3 M). Maximum dissolved weight percentage amounted to 14.33% with 3 M sulfuric acid and HCl at room temperature.

Figure 4 shows the extent of acid leaching of the ash using hot sulfuric acid (4 M) at 100°C as affected by the dissolution period up to 60 minutes. It can be seen that the dissolution extent increases with increase in the dissolution time. Complete dissolution of tin and copper in ash takes place at ≥ 50 minutes. It is also seen that

lead showed a lower dissolution extent amounting to 4%. Lead was found insoluble in the sulfuric acid solution.

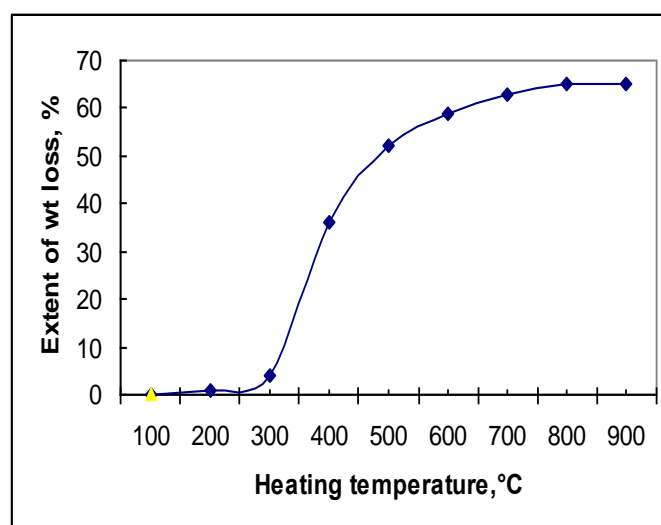


Figure2 The effect of heating temperature in air on the extent of weight loss% of printed circuit boards scrap samples

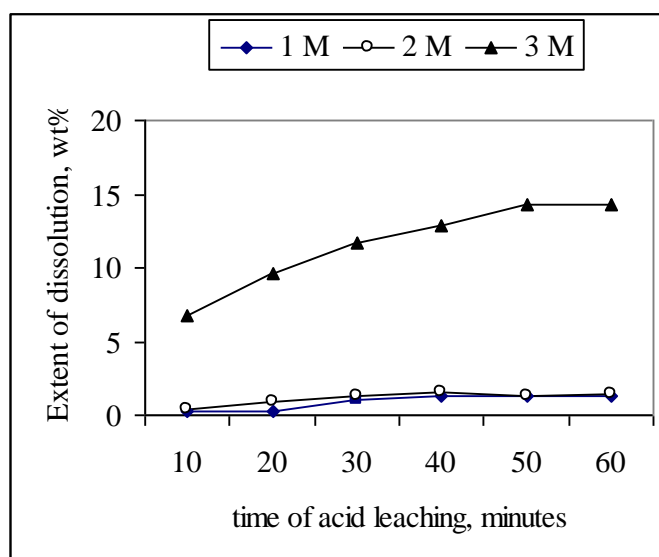


Figure 3 Effect of time of dissolution extent of ash in sulfuric acid and HCl. at room temperature.

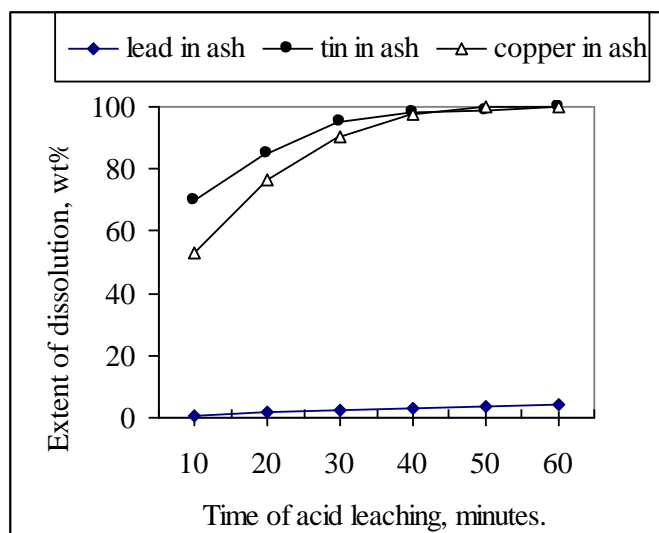


Figure 4 The extent of acid leaching of the ash using hot sulfuric acid and HCl. (4 M) at 100°C as affected by the dissolution period up to 60 minutes

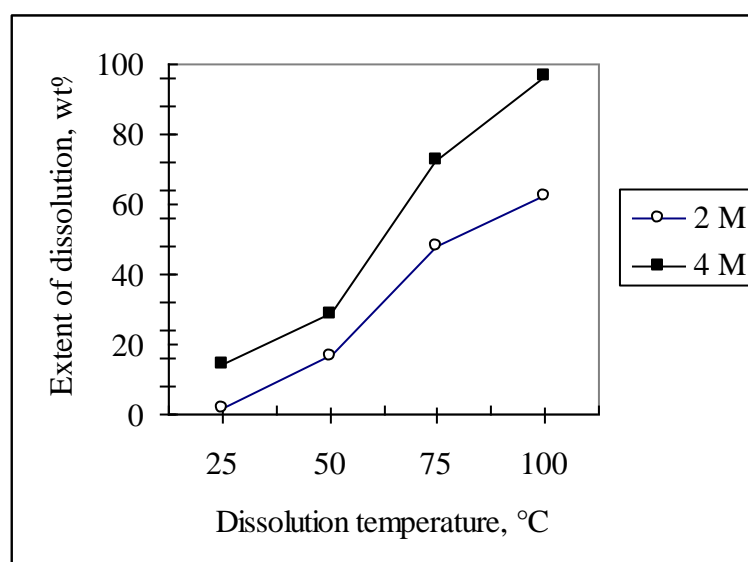


Fig. 5 Effect of dissolution temperature on the dissolution extent of copper in ash using 2 and 4 M sulfuric acid and HCl.

Figure 5 shows the effect of acid leaching temperature on the dissolution extent of copper oxide in ash using 2 and 4 M sulfuric acid after 60 minutes. It can be seen that increasing the dissolution temperature enhances the extent of dissolution. Results revealed that a maximum dissolution extent in 4M H_2SO_4 amounting to nearly 100% takes place at 90°C.

Figure 6 illustrates the effect of stirring the reacting species on the extent of dissolution. It is seen that stirring of the dissolution system enhances acid dissolution of the ash. It is seen that stirring the reaction solution at 200 rpm is found effective to completely dissolve copper present in the ash of the burnt PCB.

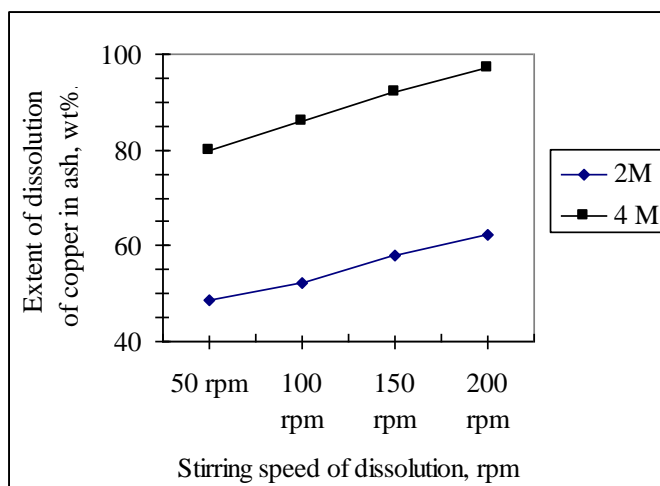


Fig. 6 Effect of stirring on the dissolution extent of copper in ash (2,4 M sulfuric acid and HCl , 100°C and 60 minutes).

3.1.2 Dissolution of the ash of the burnt PCBs in hydrochloric acid.

A set of experiments have been carried out to dissolve the ash of the burnt PCB samples in HCl acid under the same experimental conditions applied with sulfuric acid. Results revealed that a similar dissolution curves was obtained with HCl as with sulfuric acid (figures 3-6). However, the dissolution extents acquired with HCl acid are comparatively slightly lower than that attained with sulfuric acid.

3.1.3 Dissolution of the burnt PCB ash in nitric acid

Figure 7 shows the effect of nitric acid concentration on the extent of dissolution of the burnt PCB ash at 100°C. It is seen that the dissolution extent gradually increases with the corresponding increase in time approaching complete dissolution after 40 minutes with copper, 50 minutes with tin and 60 minutes with lead. It is worthy to note that after cooling the solution to room temperature, tin nitrate so obtained precipitates as basic tin oxide. Copper nitrate and lead nitrate are kept dissolved in the cold solution.

Figure 8 illustrates the effect of nitric acid concentration on the extent of dissolution of PCB ash at 100°C for 60 minutes. It is seen that the extent of ash dissolved in the acid gradually increases with increase in acid concentration. Complete dissolution takes place with 5 M nitric acid.

Figure 9 shows the effect of nitric acid concentration on the extent of copper dissolution in PCB ash at room temperature for 60 minutes. It can be seen that the weight percentage of the dissolved copper increases regularly with increase in the acid concentration.

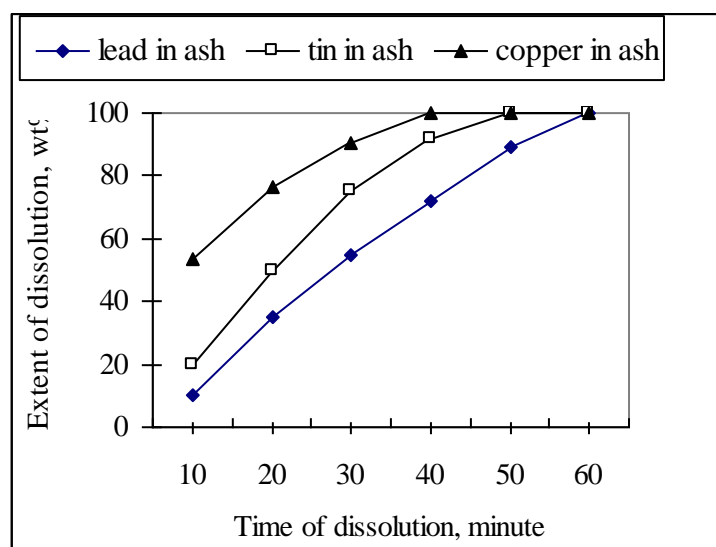


Fig. 7 Effect of time on the extent of dissolution of PCB ash in 4 M nitric acid at 100°C.

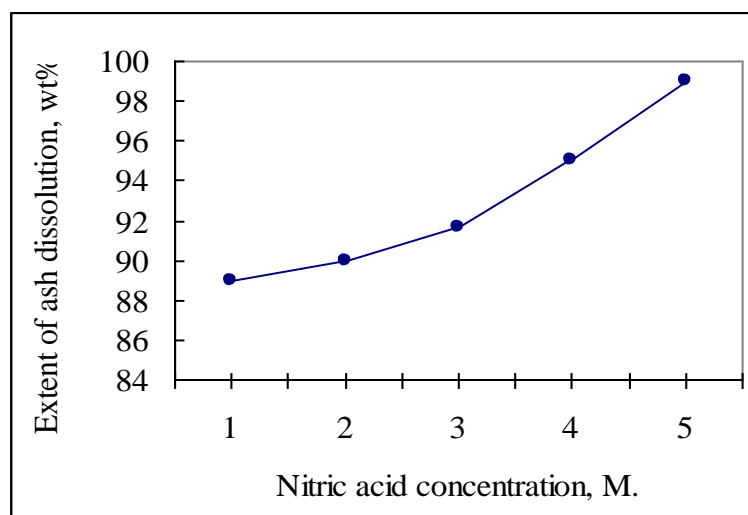


Fig. 8 Effect of nitric acid concentration on the extent of dissolution of PCB ash at 100°C for 60 minutes.

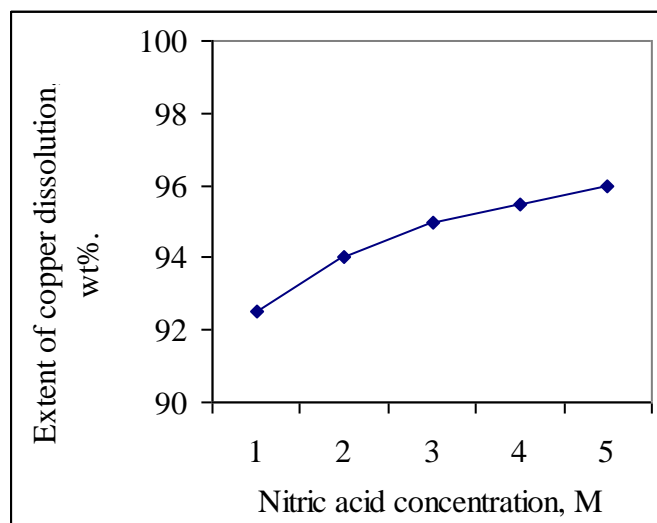


Fig. 9 Effect of nitric acid concentration on the extent of copper dissolution in the PCB ash at room temperature.

3.2 Extraction of metals from the un-burnt PCBs by hydrometallurgical treatment.

3.2.1 Leaching in nitric acid

Figure 10 shows the dissolution extent of the un-burnt PCB samples (types **a** and **c4**) in 1 M nitric acid as a function of leaching time up to 100 minutes at room temperature. It can be seen that the weight percentage per unit area of the dissolved copper is insignificant (0.34 %) after 10 minutes and 0.347 % after 100 minutes.

Figures 11 and 12 show the extent of copper dissolved in 2 M and 3M nitric acid, respectively as a function of leaching time up to 100 minutes at room temperature.

It can be seen that the extent of dissolved copper increases gradually with increase in time up to 60 minutes approaching more or less a constant value.

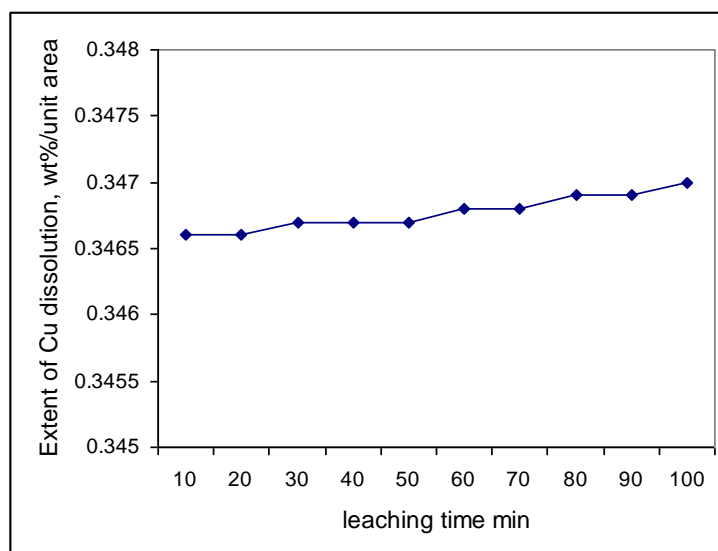


Fig 10 Effect of leaching time on the extent of copper dissolution in 1 M nitric acid at room temperature (no stirring)

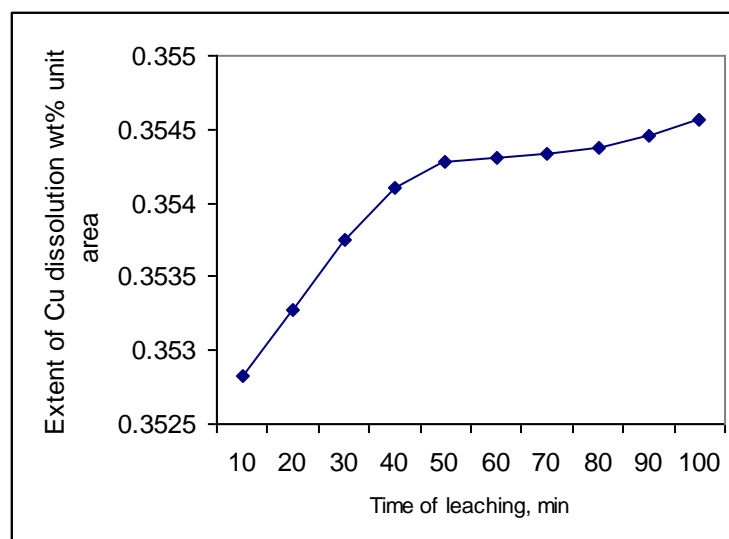


Fig 11 Effect of leaching time on the extent of copper dissolution in 2 M nitric acid at room temperature (no stirring)

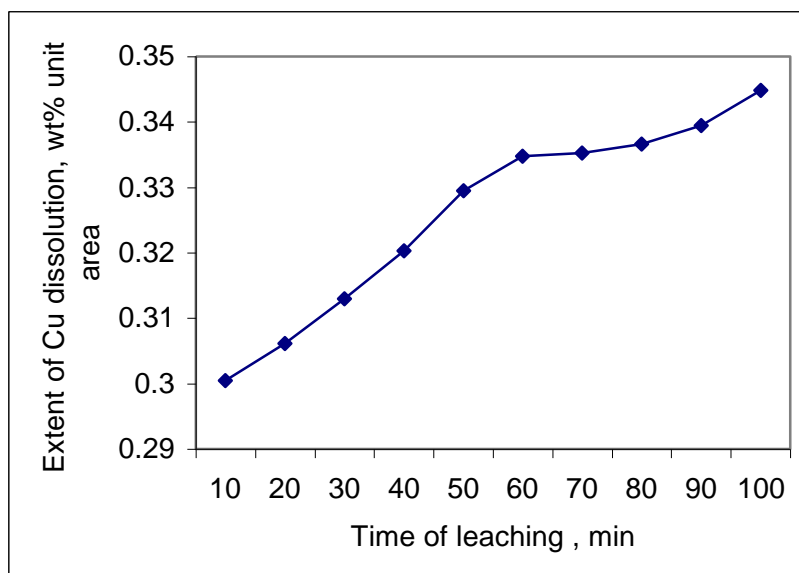


Fig 12 Effect of leaching time on the extent of copper dissolution in 3 M nitric acid at room temperature (no stirring)

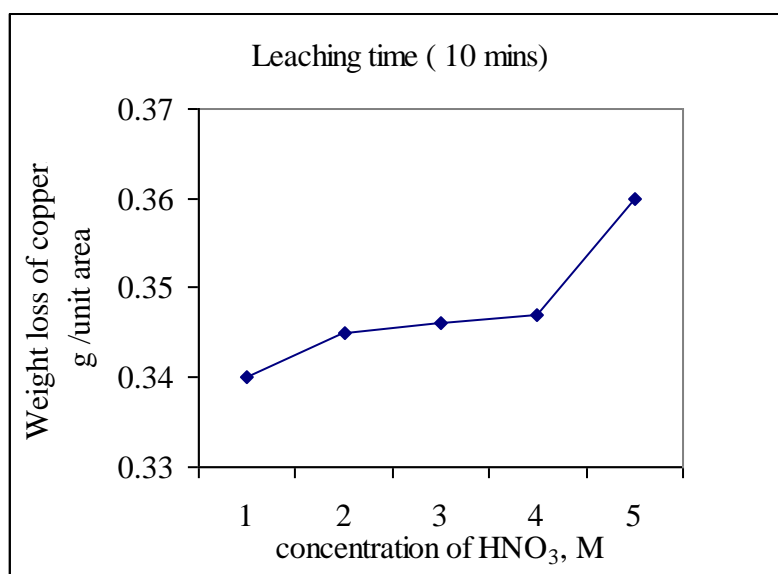


Fig. 13 The effect of nitric acid molarity on the extent of the dissolved copper at room temperature.

Figure 13 shows the effect of nitric acid concentration on the weight of copper dissolved in the acid solution at room temperature. It can be seen that the extent of the dissolved copper slightly increases with increase in nitric acid molarity.

Figure 14 shows the extent of dissolution of copper in 2 M nitric acid at 25, 50 and 75°C for periods up to 100 minutes. It can be seen that increasing leaching temperature enhances the extent of dissolution of the metal. However, complete dissolution takes place after 60 and 90 minutes at 50°C and 75°C, respectively.

Figure 15 illustrates the extent of copper dissolved in 4 M nitric acid a function of leaching time up to 100 minutes at 50°C and 75°C. It can be seen that the extent of dissolved copper increases with increase in temperature. Complete dissolution takes place at 75°C and 50°C after 60 and 90 minutes, respectively.

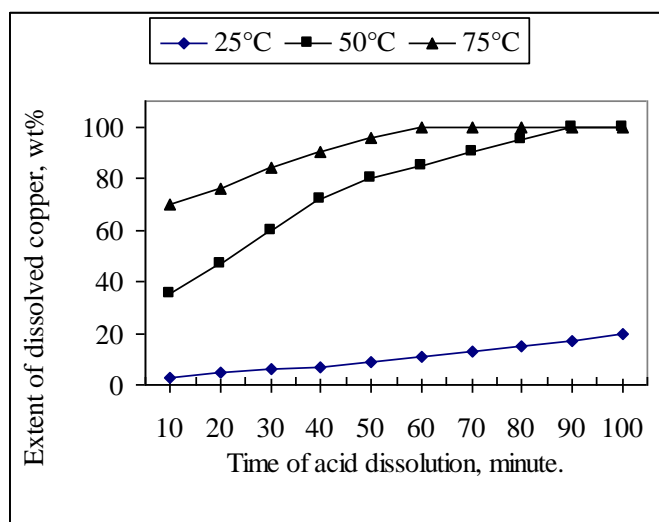


Figure 14 Effect of time on the extent of copper dissolution in 2 M nitric acid at temperatures up to 75°C.

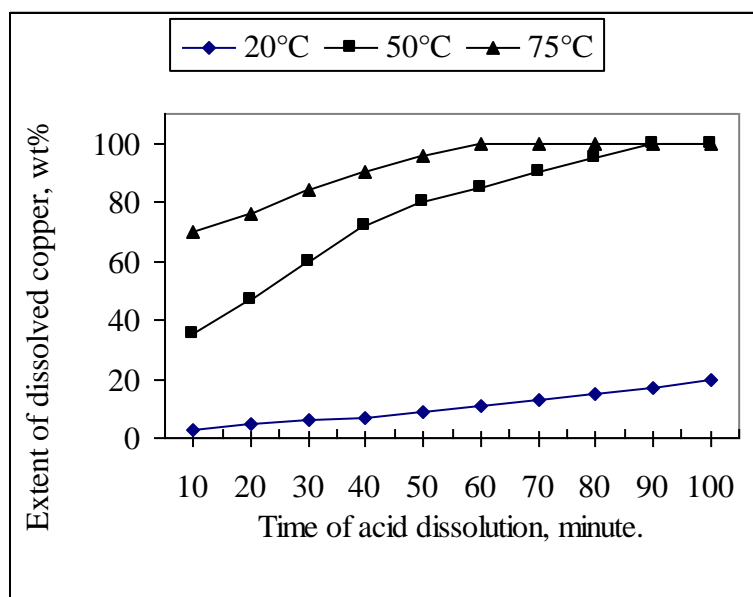


Fig 15 The effect of leaching time on the extent of copper dissolution in 4 M nitric acid at different temperatures up to 75°C.

Figure 16 shows that about 50% of lead dissolved in 2M nitric acid at 20°C and after 60 minutes. The metal dissolved more readily at higher temperature (100°C) whereby complete dissolution takes place after ≥ 50 minutes.

Figure 17 shows the effect of dissolution temperature on lead dissolution in 2M nitric acid for periods up to 60 minutes. It can be seen that the extent of dissolution increases linearly with increase in temperature and time. Maximum extent of dissolution is attained at 100°C for period ≥ 50 minutes.

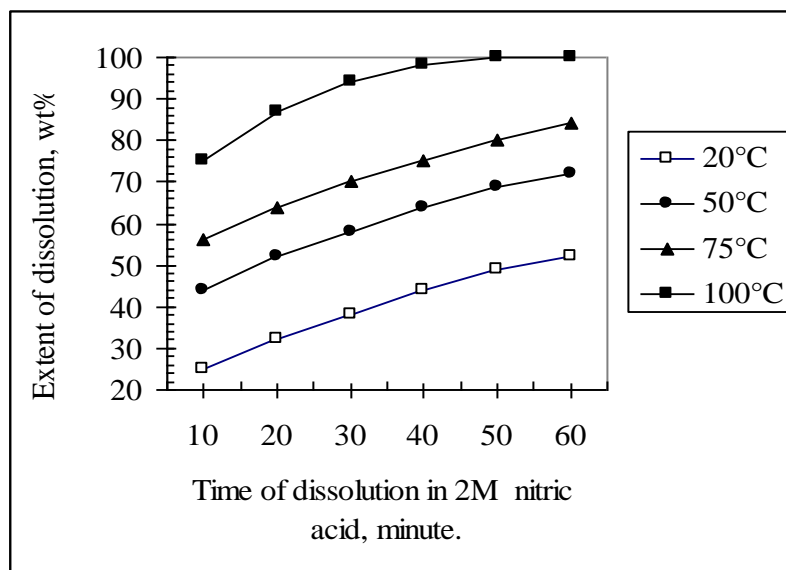


Figure 16 The effect of time and temperature on the dissolution extent of lead in 2 M nitric acid.

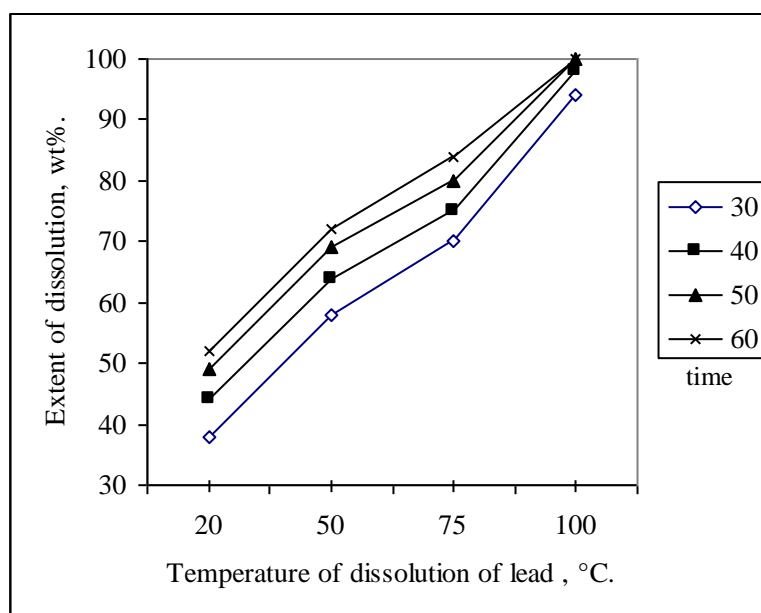


Fig. 17 Effect of temperature on the extent of dissolution of lead in 2M nitric acid for periods up to 60 minutes.

Figure 18 shows the extent of dissolution of tin as a function of nitric acid molarity at room temperature and after 100 minutes. It can be seen that tin is sparingly soluble at room temperature so that only 2.2 % of the metal dissolves in 5M nitric acid after 100 minutes.

Figure 19 shows the effect of temperature on the extent of tin dissolution in nitric acid having different molarities up to 5M and for 60 minutes. It can be seen that the extent of dissolution of tin increases slowly with increase in both temperature up to 50°C and acid molarity. However, tin dissolution increases drastically with the corresponding increase in temperature up to 100°C attaining complete dissolution extent at 100°C with nitric acid having $\geq 2\text{M}$ concentration

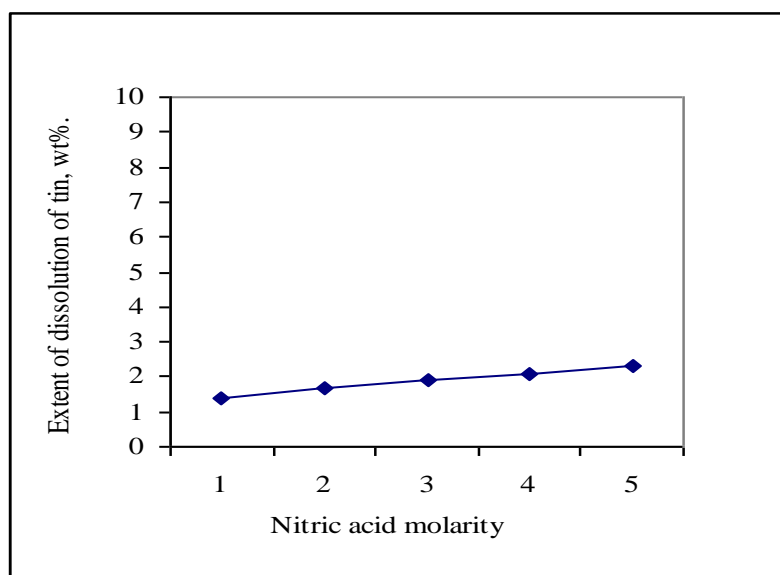


Figure 18. The effect of nitric acid molarity on extent of tin dissolution at room temperature and after 100 minutes..

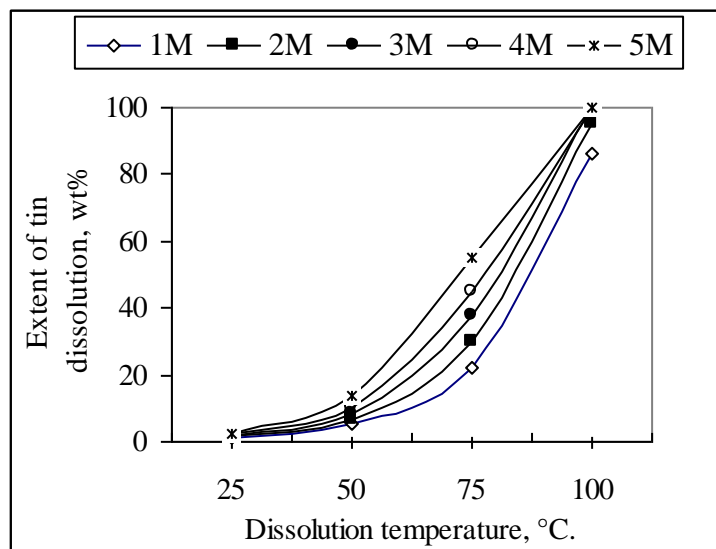


Figure 19 Effect of temperature on the extent of tin recovery in nitric acid.

Figure 20 illustrates that at one and the same temperature, tin dissolution increases with increase in nitric acid concentration. The acid attack is pronounced at 100°C and becomes less effective at lower temperatures. It is worthy to note that when the hot tin solution was cooled down to room temperature, a white solid tin oxynitrate precipitates. Figure 21 shows the effect of temperature on the extent of tin oxynitrate deposition. It can be seen that the critical temperature for tin oxynitrate separation from the hot acidic solution is below 50°C.

Figure 22 shows the extent of dissolution of copper, lead and tin in 4M nitric acid at 50°C for periods up to 60 minutes. It can be seen that the extent of dissolution of these metals slightly increases with time up to 30 minutes approaching more or less a constant value (4% and 6% respectively) up to 60 minutes. With copper, the extent of dissolution is comparatively higher in magnitude as compared to both lead and tin.

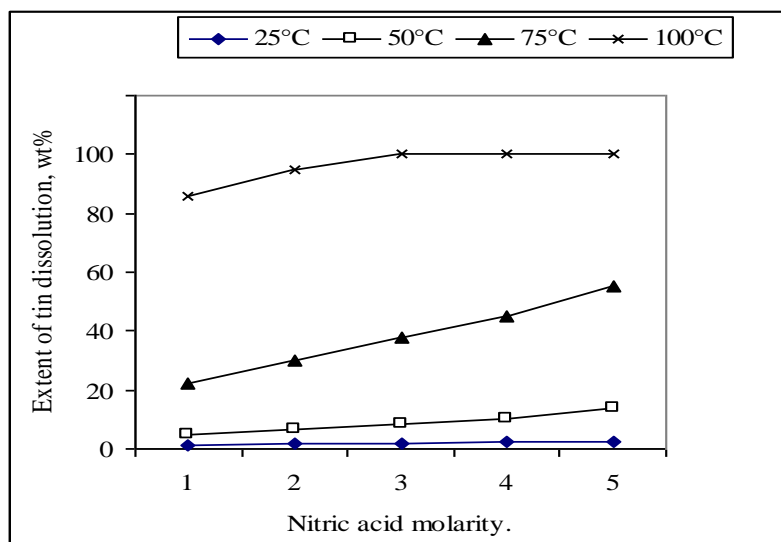


Fig. 20 Effect of nitric acid molarity on the extent of tin dissolution at temperatures up to 100°C.

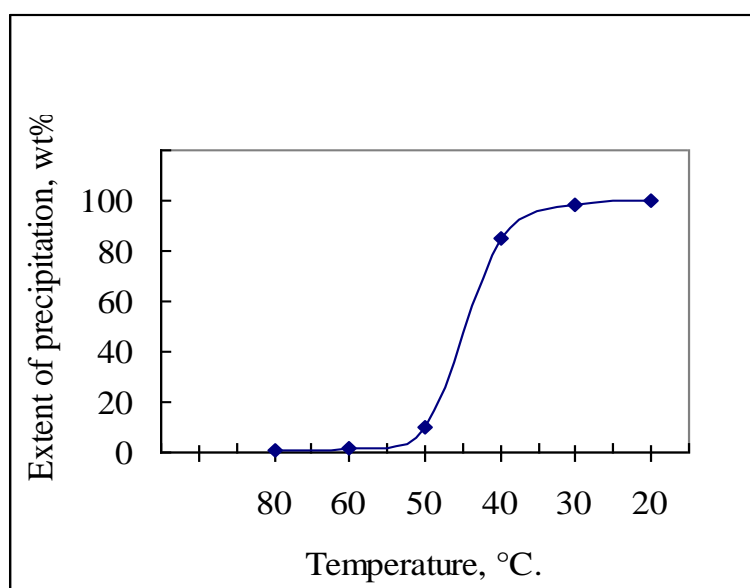


Figure 21 Effect of temperature on the extent of deposition of tin oxynitrate.

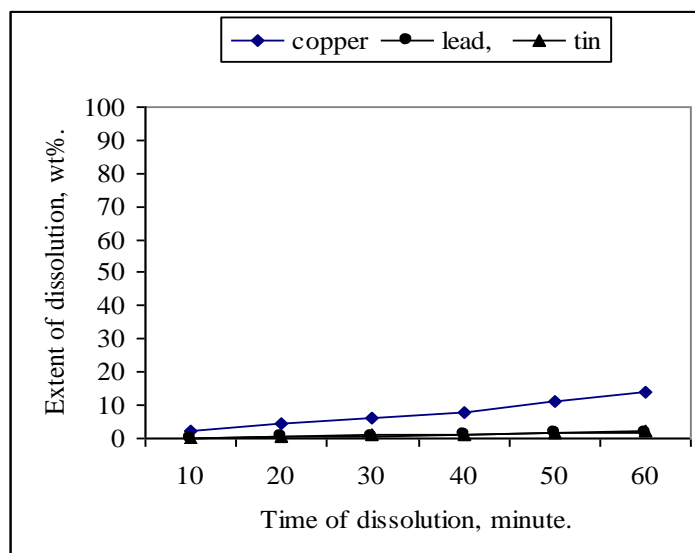


Figure 22 Extent of dissolution of Cu, Pb and Sn as affected by time in 4M nitric acid at 20°C. (higher stoichiometric ratio.

3.2.2 Leaching in sulfuric acid

Figure 23 the dissolution extent of copper present in the un-burnt PCBs in sulfuric acid having different concentration for 60 minutes. Experiments were carried out at temperatures up to 100°C. It can be seen that the extent of copper dissolution is negligible at room temperature. At higher temperatures and at 50°C, the extent of dissolution becomes more significant. Copper dissolution in ≥ 6 mol sulfuric acid becomes aggressive at temperatures $\geq 75^\circ\text{C}$. It is worthy to note that during copper dissolution in 10 M sulfuric acid, overheating of the system takes place so that cooling becomes necessary to prevent flash of the reacting fluid.

Figure 24 shows the effect of stoichiometric ratio of sulfuric acid having different concentrations on the extent of dissolution of a copper sample at 100°C for 60

minutes. It is seen that, for one and the same concentration of the reacting sulfuric acid, the extent of dissolution increases gradually with increase in stoichiometric ratio. Maximum extent of copper dissolution in 10M sulfuric acid is attained at ≥ 1.20 stoichiometric ratio. However, the maximum extent of copper dissolution can be attained with 8 M sulfuric acid.

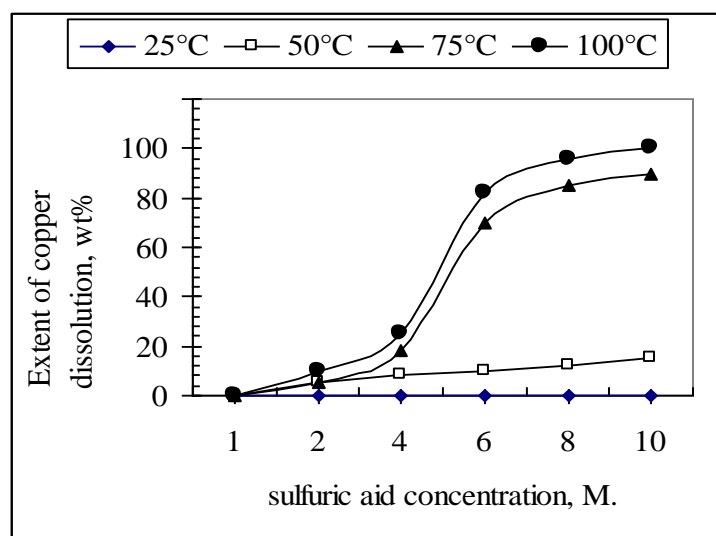


Figure 23 Effect of sulfuric acid concentration on the extent of dissolution of copper at temperatures up to 100°C (1.25 stoichiometric ratio)

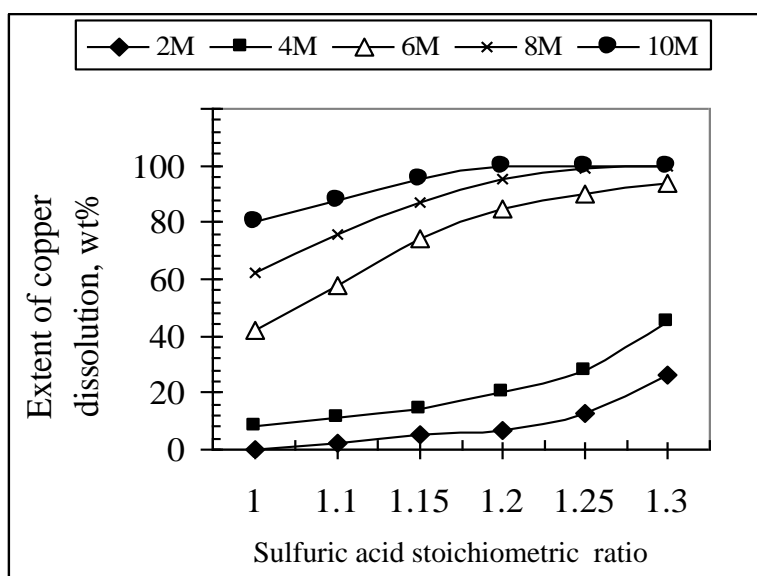


Figure 24 Effect of stoichiometric ratio of 2M-10M sulfuric acid on the extent of dissolution of copper at 100°C.

Figure 25 represents the effect of stoichiometric ratio of sulfuric acid on the extent of recovery of copper at 75°C. It can be seen that the extent of recovery increases linearly with increase in the stoichiometric ratio of 4 M sulfuric acid.

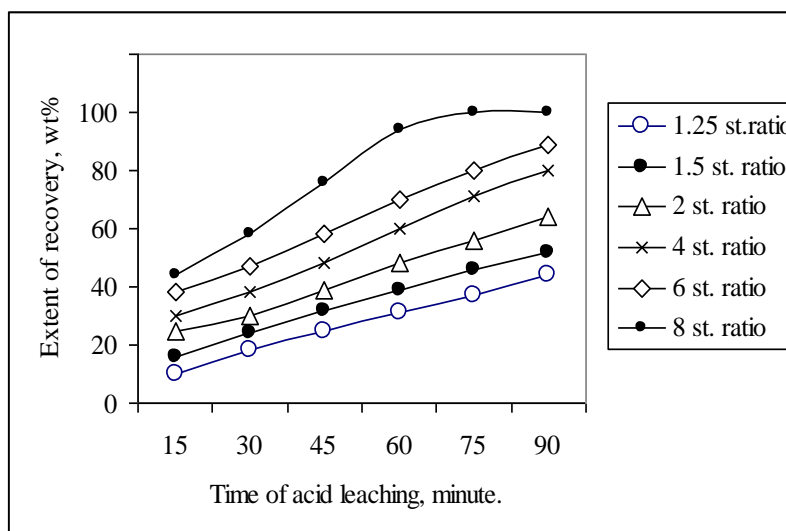


Fig. 25 Effect of stoichiometric ratio of 4 M sulfuric acid on the extent of copper recovery from spent PCBs.

The effect of sulfuric acid used for leaching copper from the PCBs on the polymer base material was studied. Figure 26 shows the extent of deformation of the polymer base material as affected by the acid concentration up to 10 mol concentration and at different temperatures up to 100°C for 15 minutes. It is seen that the base material is stable against the attack of 2M acid and at lower temperature. The polymer base starts gradual deformation with the increasing the acid concentration up to 10 mol. It is worthy to note that the polymer material completely deformed at 100°C and with acid concentration > 8 mol.

Figures 27 and 28 show the extent of deformation of the polymer base-material as affected by the nitric and HCl acids, respectively. Experiments were carried out

using up to 6 mol concentration and at different temperatures up to 100°C for 15 minutes. It is seen in Fig. 27 that the base material is chemically stable against the attack of 2M acid at lower temperatures. The polymer base manifests gradual deformation with increasing the acid concentration up to 4 mol. Figure 28 illustrates the extent of polymer deformation in weight percentage as a function of HCl acid concentration. The acid effect was carried out at temperatures up to 100°C. It can be seen that HCl acid has no degradation effect on the base material at lower temperatures and low concentration. However, acid attack becomes pronounced with increasing temperature up to 100°C. The polymer material deformed completely at 100°C and with 4M acid concentration

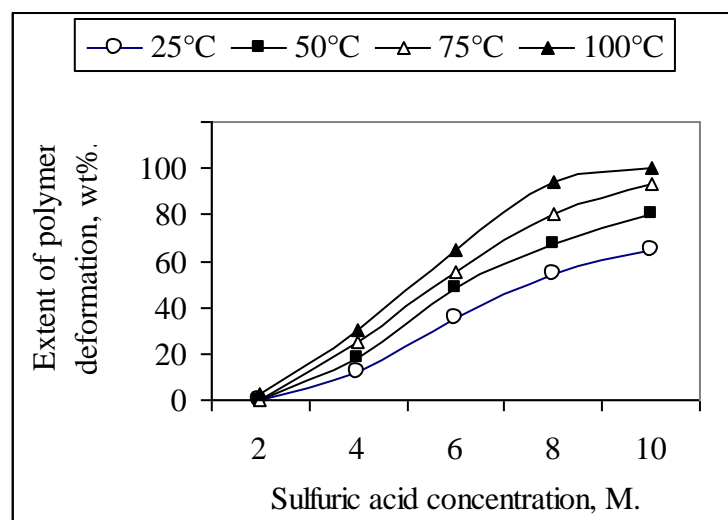


Figure 26 The effect of sulfuric acid concentration on the extent of polymer deformation at different temperatures

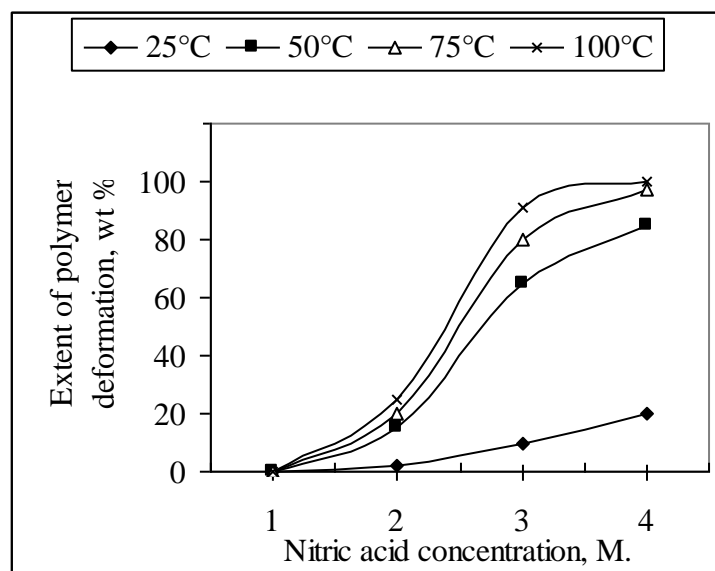


Figure 27 Effect of nitric acid concentration on the extent of deformation of the polymer base-material of PCBs at temperatures up to 100°C.

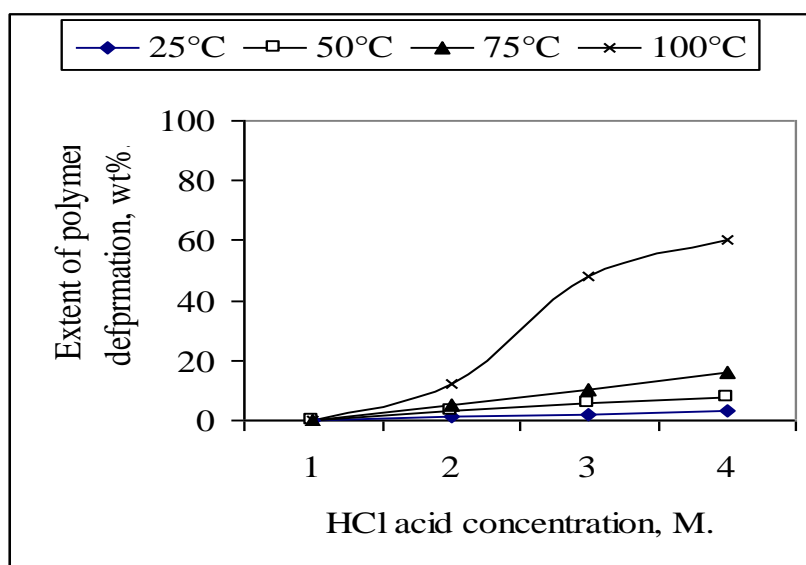


Fig. 28 The effect of HCl acid concentration on the extent of deformation of the polymeric base-material of PCBs at temperatures up to 100°C.

3.2.3 Recovery of gold from PCBs samples type C

Figure 29 shows the results of gold recovery from the PCB type c using nitric acid having 0.5 – 2 M concentration at room temperature and for periods up to 50 minutes.

It can be seen that the weight of gold recovered from the PCBs was insignificant by leaching with dilute nitric acid. This result was also confirmed by using the same acid having a concentration range 0.5-2M. The weight of the recovered gold was found poor particularly within the early periods of acid treatment and up to 25 minutes. Leaching of the PCB with more concentrated nitric acid, ≥ 2 M, has proven to recover gold at high extent. A pronounced recovery weight of gold takes place and increases gradually with increase in time for periods >40 minutes.

The same experiments were conducted at 100°C for 30 minutes. Figure 30 illustrates the results obtained under these conditions. It is seen that the weight of the recovered gold increases drastically with increase of the nitric acid concentration from 0.5 M to 1M. The extent of the weight of gold then increases slightly with further increase of the acid concentration. Complete recovery of gold takes place using ≥ 1.5 M nitric acid at 100°C and for 30 minutes. Figure 31 illustrates the weight recovered of gold by leaching the PCBs using 2 M nitric, sulfuric and hydrochloric acids at 100°C. It can be seen that the extent of gold recovery increases in the order nitric, sulfuric and hydrochloric acid. With sulfuric and HCl acids, the extent of recovery was poor even after 60 minutes. Determination of the extent of gold recovery using sulfuric acid amounts to about 14%.

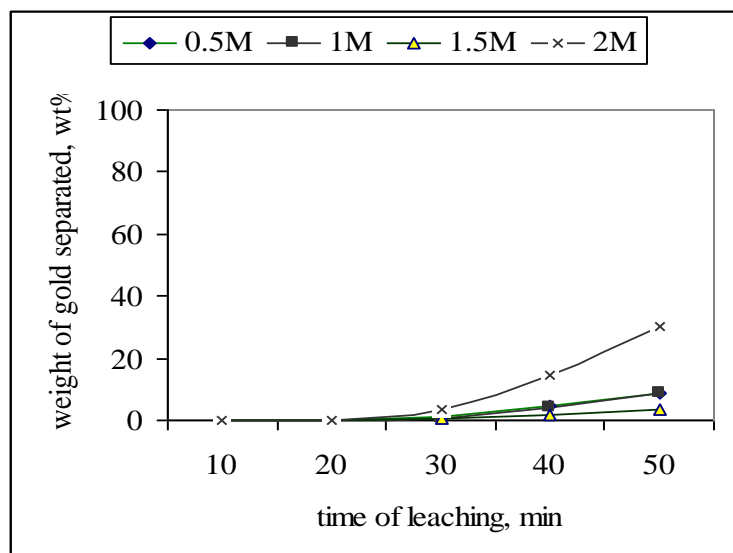


Figure 29 Effect of time of leaching using nitric acid (0.5 – 2 M) on the weight of gold separated from the PCB sample (room temperature).

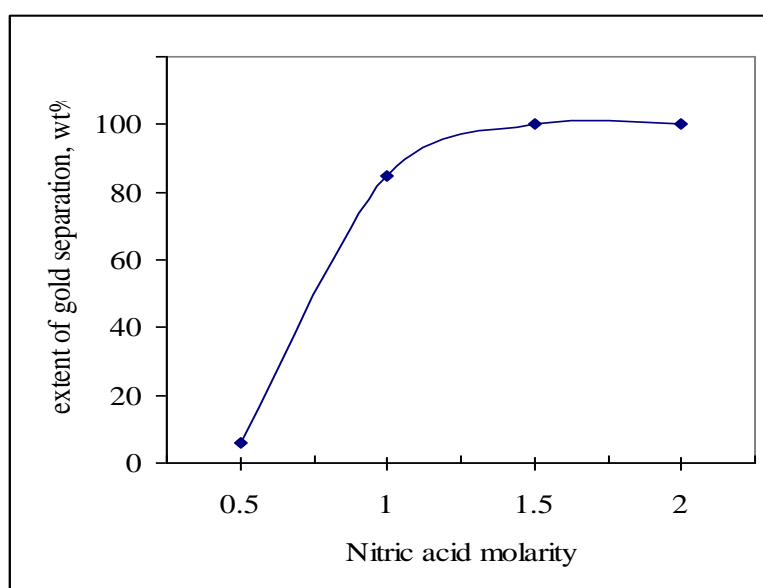


Figure 30 effect of nitric acid (0.5 – 2 M) on the weight of gold recovered from the PCB sample at 100°C for 30 minutes.

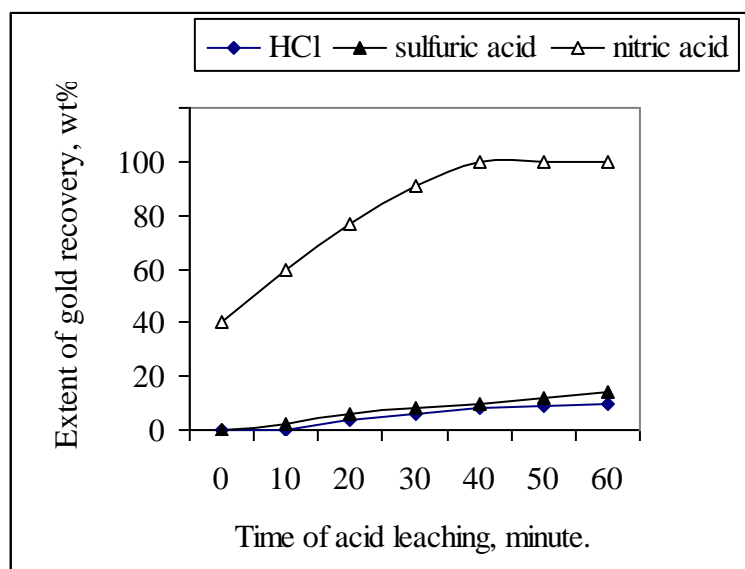


Figure 31 Effect of leaching time on the extent of recovery of gold using 2M acids at 100°C.

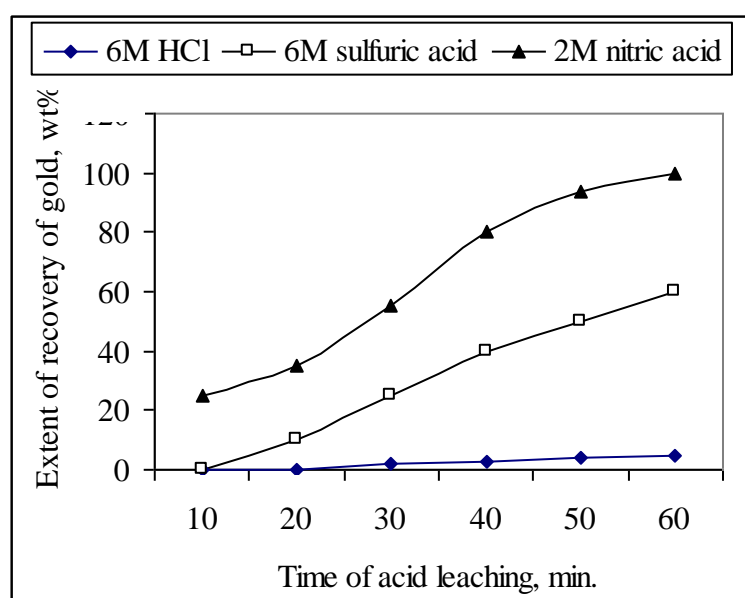


Figure 32 Effect of leaching time on the extent of recovery of gold using 2-6 M acids at room temperature.

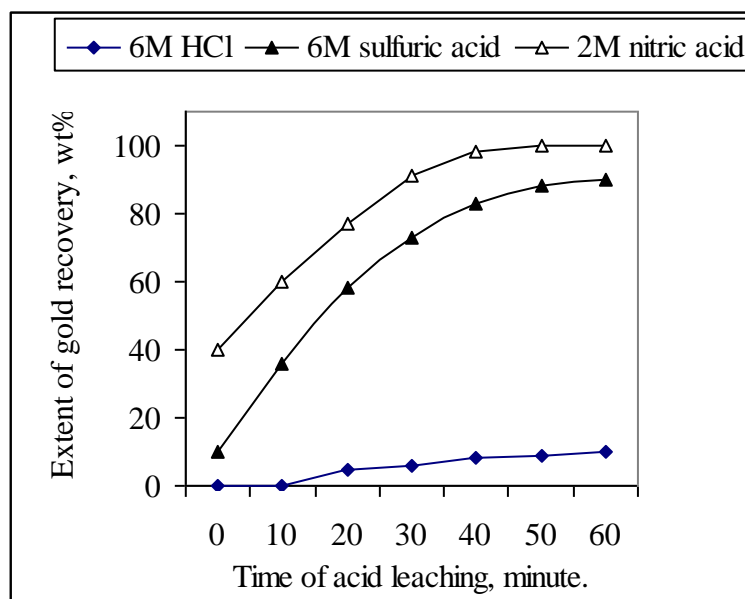


Figure 33 Effect of leaching time on the extent of recovery of gold using 2-6 M acids at 100°C.

Another set of experiments were performed using more concentrated sulfuric and HCl acids at room temperature. Results are graphically represented by the curves shown in Fig32. Figure 33 shows the extent of gold recovery using 2M nitric, 6M sulfuric and 6M HCl acids at 100°C for periods up to 60 minutes. It is seen that the extent of gold recovery increases more readily with increase in leaching time approaching a maximum value after 60 minutes. Hot leaching is more pronounced as compared with leaching at room temperature

3.3 Thermal reduction of copper, tin and Lead oxides

Copper sulfide, basic tin oxide and lead chloride were washed and dried before the reduction process. Free metals have been recovered by thermal reduction of their respective oxides using hydrogen gas or carbon. Precipitated basic tin oxide was first refined before reduction by heating at temperatures up to 1000°C.

Figure 34 shows the tin oxide purity as a function of the heating temperature. It can be seen that the amount of loss on ignition increases gradually with increase in temperature approaching a constant value of 19.3% at $\geq 900^{\circ}\text{C}$. Tin purity as high as 99.995 % by weight, was attained after heating at $>1000^{\circ}\text{C}$.

Figure 35 shows the extent of copper sulfide reduction using hydrogen gas as a function of temperature. It can be seen that reduction process of copper sulfide started at $> 600^{\circ}\text{C}$. At 700°C , the extent of reduction increases gradually up to about 46 %. This value is kept constant up to 900°C . With further increase in reduction temperature, a rapid increase in the extent of reduction takes place. Complete reduction of copper sulfide is attained at 1250°C . It is worthy to note that the part of the curve within the temperature range $600\text{-}700^{\circ}\text{C}$ has the same slope of the part displayed within the temperature range $1000\text{-}1250^{\circ}\text{C}$.

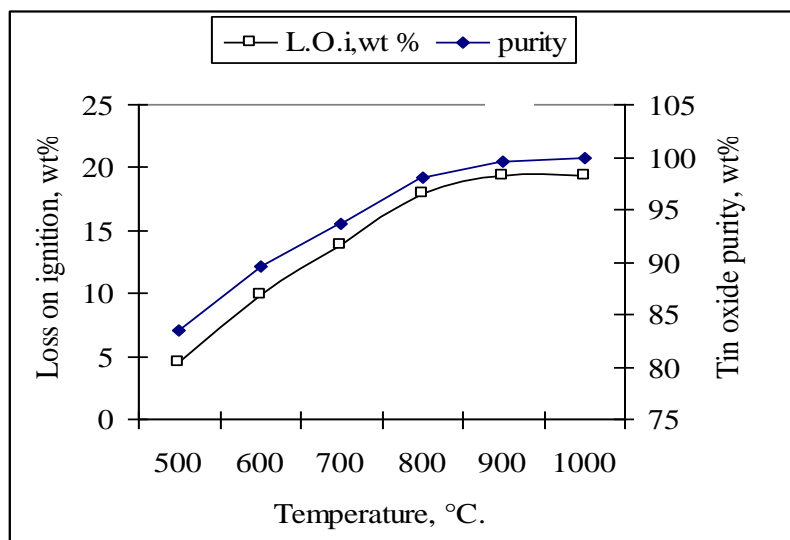


Fig. 34. Effect of temperature on the purity extent of the deposited tin oxide.

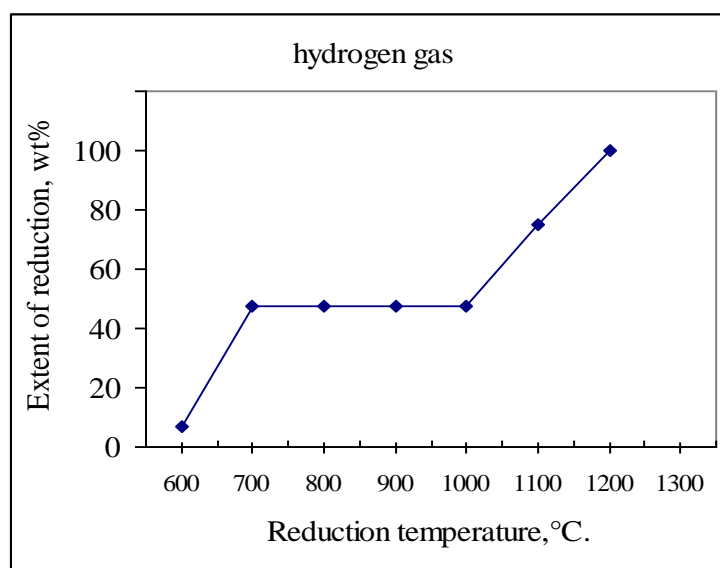


Fig. 35 Effect of reduction temperature on the extent of reducing copper sulfide using hydrogen gas.

Figure 36 illustrates the reduction curve of lead oxide as affected by temperature using hydrogen gas as a reducing agent.. It can be seen that the reduction process commenced at temperature $>500^{\circ}\text{C}$. The extent of reduction increases linearly with increase in temperature. Complete reduction is attained at 950°C . Figure 37 shows

the Arrhenius plot for the thermal reduction process of lead oxide with hydrogen gas.

Figure 38 shows the reduction extent of copper, tin and lead oxides as a function of reduction temperature using carbon as a reducing agent. It can be seen that the temperature at which the reduction process starts increases in the order: lead, tin and copper. Complete reduction with lead is attained at 900°C. The corresponding temperature recorded for tin and copper amounts to 1050°C and 1200°C, respectively.

Figure 37 shows the Arrhenius plot for the thermal reduction process of lead oxide using hydrogen gas. Figure 39 illustrates the Arrhenius plot for the thermal reduction process for the three metals using carbon. The calculated ΔE value amounts to 51.16 kJ/mole, 52.50 kJ/mole and 29.2 kJ/mole for copper oxide, CuO, lead oxide, PbO and tin oxide SnO, respectively. Figure 40 shows the purity extent of the separated gold strips as a function of potassium persulfate: sulfuric acid mol ratio. It can be seen that pure gold is obtained by fluxing the removed gold strips with boiling concentrated sulfuric acid containing ≥ 0.2 mol ratio of potassium persulfate : sulfuric acid.

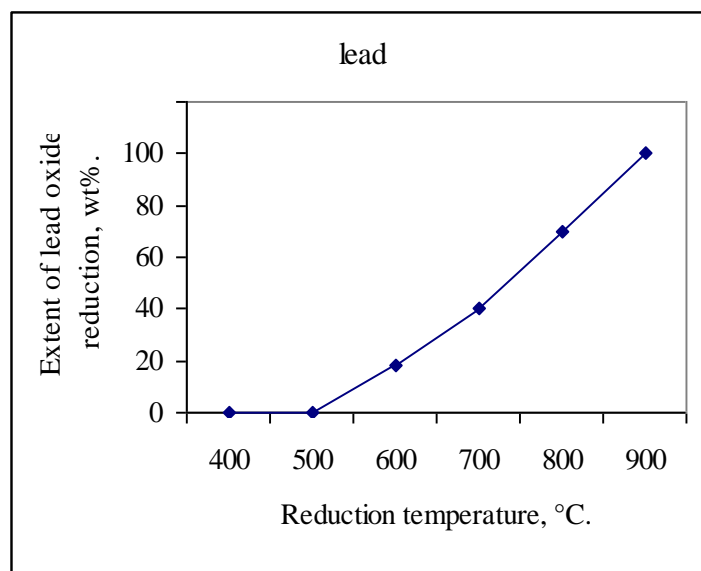


Fig. 36 Effect of reduction temperature on the extent of reducing lead oxide using hydrogen gas.

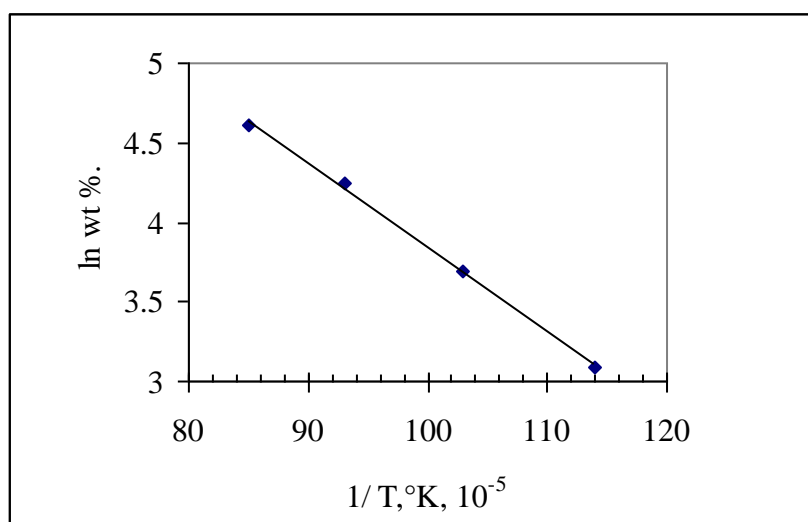


Fig. 37 The Arrhenius plot for the thermal reduction process of lead oxide.

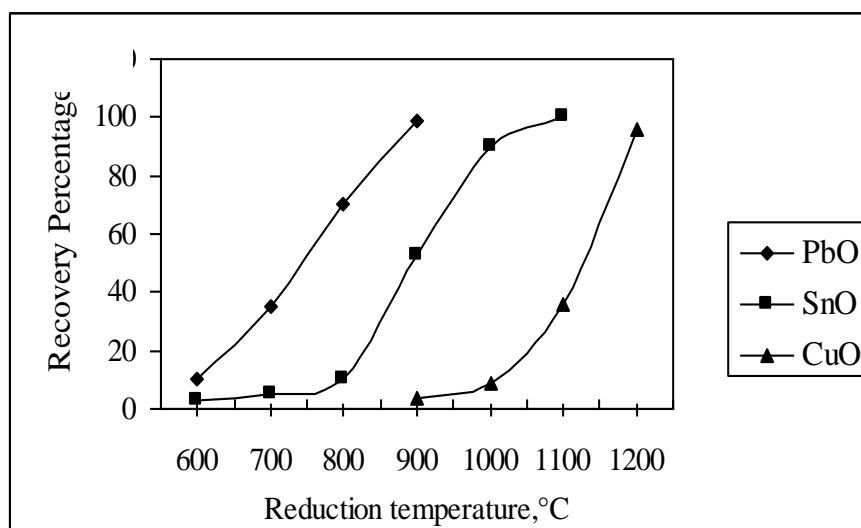


Fig. 38 Effect of temperature on the extent of reduction of copper, lead and tin using carbon as a reducing agent.

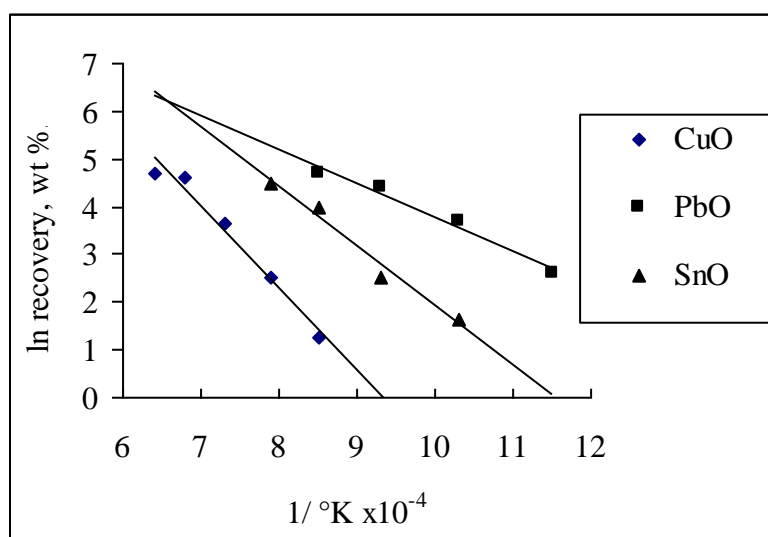


Fig. 39 The Arrhenius plot for the thermal reduction process of copper, lead and tin oxides.

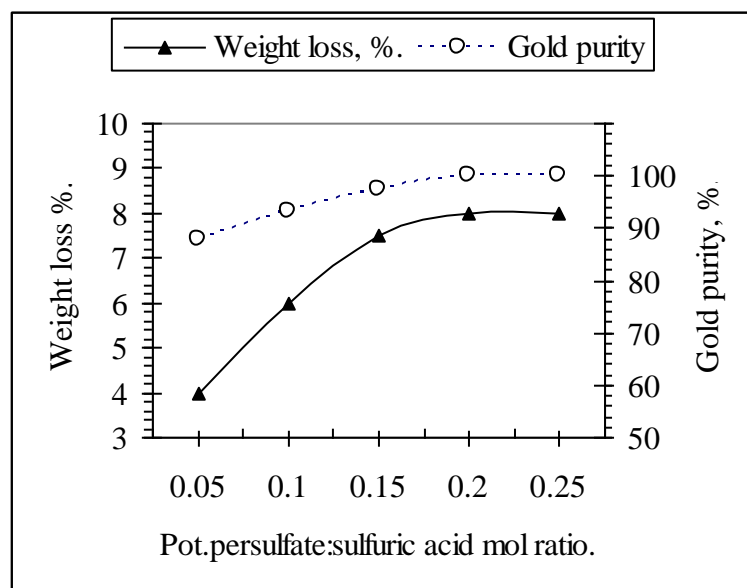


Fig. 40 The purity extent of the separated gold strips as a function of potassium persulfate: sulfuric acid mol ratio.